

# DNA response and repair gene mutations as a signature for pembrolizumab response in never-smoker non-small lung cancer: real word approach and patient similarity network analysis

**Marco Filetti**

Sapienza University of Rome

**Mario Occhipinti** (✉ [mario.occhipinti@uniroma1.it](mailto:mario.occhipinti@uniroma1.it))

Sapienza University of Rome

**Alessio Cirillo**

Sapienza University of Rome

**Fabio Scirocchi**

Sapienza University of Rome

**Alessio Ugolini**

Sapienza University of Rome

**Raffaele Giusti**

St. Andrea Hospital

**Pasquale Lombardi**

Fondazione Policlinico Universitario Agostino Gemelli, IRCCS

**Gennaro Daniele**

Fondazione Policlinico Universitario Agostino Gemelli, IRCCS

**Andrea Botticelli**

Sapienza University of Rome

**Giuseppe Lo Russo**

Fondazione IRCCS Istituto Nazionale dei Tumori

**Filippo Maria Braud**

University of Milan

**Paolo Marchetti**

IDI-IRCCS

**Marianna Nuti**

Sapienza University of Rome

**Elisabetta Ferretti**

Sapienza University of Rome

**Lorenzo Farina**

Sapienza University of Rome

**Aurelia Rughetti**

Sapienza University of Rome

**Manuela Petti**

Sapienza University of Rome

---

## Research Article

**Keywords:** immunotherapy, DDR, NSCLC, never-smoker, network analysis

**Posted Date:** March 10th, 2023

**DOI:** <https://doi.org/10.21203/rs.3.rs-2651331/v1>

**License:**   This work is licensed under a Creative Commons Attribution 4.0 International License.

[Read Full License](#)

---

# Abstract

## Purpose

Single-agent immune checkpoint inhibitor (IO) therapy is the standard of care for non-oncogene addicted advanced non-small cell lung cancer (aNSCLC) with PD-L1  $\geq 50\%$ . High tumor mutation burden (H-TMB) is a notable biomarker for IO response. Smoking-induced harm generates H-TMB in smoking aNSCLC patients (S-pts), whereas never-smoking patients (NS-pts) usually have low TMB and are IO-unresponsive. However, NS-pts with H-TMB have not been well molecularly characterized.

## Experimental design

Clinical data of 142 aNSCLC patients with PD-L1  $\geq 50\%$  treated with first-line pembrolizumab were retrospectively collected. Next-generation sequencing was performed using the FoundationOne®CDx assay to correlate genomic alterations with clinical characteristics and response outcomes. Detected mutations were classified into eleven main pathways: cell cycle, Hippo, Myc, Notch, oxidative stress/Nrf2, PI3K, RTK/RAS/MAP, TGF- $\beta$ , p53, b-catenin/Wnt, and DDR. Enrichment analysis was performed on pathways with at least one mutation per patient to characterize patient subgroups based on mutated pathways. Moreover, to further investigate the molecular characterization of patients' subgroups, we built and analyzed the patient similarity network exploiting the mutational profile to compute the pairwise similarity between patients.

## Results

There were 111 S-pts and 31 NS-pts; S-pts had higher TMB (median TMB: 8 vs. 4 Mut/Mb). However, 11 NS-pts had high TMB (median TMB: 16.39 Mut/Mb) and were significantly enriched in b-catenin/Wnt and DDR pathway mutations (p-values=0.0027 and 0.0014, respectively) compared to others and H-TMB/S-pts. Using publicly available molecular characterization data (of 853 NSCLC patients from 2 randomized controlled trials), DDR pathway mutations were confirmed to be enriched in NS-pts with H-TMB. In the real world cohort the subgroup of H-TMB/NS-pts with DDR pathway mutation showed better IO response and survival. Moreover, the similarity network analysis of the NS-pts revealed the presence of one subgroup characterized by high TMB, improved OS and a prevalence of DDR pathway mutations.

## Conclusions

DDR signature has a potential role as additional generator of H-TMB in NS-pts. This subgroup of IO-responsive NS-pts may have better prognosis.

## Introduction

Pembrolizumab is the standard of care for stage IV, non-oncogene addicted advanced non-small cell lung cancer (aNSCLC) with programmed death-ligand 1 (PD-L1)  $\geq 50\%$  (1). However, the degree of benefit

associated with pembrolizumab is variable, and identifying biomarkers for response other than PD-L1 expression remains a challenge.

Tumor mutation burden (TMB), defined as the total number of nonsynonymous mutations per sequenced coding area of a tumor genome, has emerged as a tumor attribute associated with immunotherapy (IO) efficacy across different tumor types (2). Ricciuti et al. recently demonstrated that increasing TMB levels are associated with immune cell infiltration and inflammatory T-cell-mediated response; in aNSCLC, this results in increased sensitivity to PD-1/PD-L1 blockers across PD-L1 expression subgroups (3). Smoking-induced harm is a mechanism that generates a high TMB (H-TMB) in aNSCLC smoking patients (S-pts). In contrast, never-smoking patients (NS-pts) usually have a low TMB (L-TMB) and are generally considered to have a reduced responsiveness to IO (4).

In this context, various signaling pathway mutations have been proposed as predictors of response or resistance to IO. For example, cell cycle alterations (i.e., MDM2/MDM4 amplifications) have been possible candidate markers of IO resistance (5). Conversely, alterations in DNA damage response and repair (DDR) genes are associated with higher genomic instability and H-TMB in cancer; this may enhance immunogenicity via an increased tumor-specific neoantigen load (6–9). Deleterious DDR mutations are frequent in aNSCLC and are associated with improved clinical outcomes in patients treated with PD-L1 blockade (10).

In this paper, we investigated the potential role of signaling tumor pathway mutations, combined with TMB and clinical features, on response outcomes in a real-world population of aNSCLC treated with pembrolizumab.

## Materials And Methods

### Real-world cohort

This retrospective study was conducted at the Sapienza University of Rome, Italy. The internal review boards and local ethics committees approved the study protocol (Protocol number: 297 SA\_2019). Patient data were collected in conformance with the principles of the Declaration of Helsinki, Good Clinical Practice guidelines, and local ethical rules. All patients provided written informed consent for use of their clinical data (at any point in their medical history) for research.

The collected variables included: age, Eastern Cooperative Oncology Group performance status score (ECOG PS), gender, ethnicity, smoking history, diagnosis, histology, tumor burden and metastatic sites, comorbidities, and start and end date of treatment. Data from 142 consecutive aNSCLC patients were collected retrospectively between January 2017 and March 2021. The following criteria had to be met for inclusion in the study:

1. Cytological or histological diagnosis of advanced NSCLC (stage IIIB to IV)
2. Receipt of at least one cycle of first-line pembrolizumab

3. ECOG PS score of 0–2

4. Availability of tumor tissue for next generation sequencing (NGS) analysis

The patients' clinical characteristics have been summarized in Table 1. Treatment was continued until the occurrence of disease progression, unacceptable toxicity, withdrawal of consent, or death. Treatment beyond progressive disease was permitted in cases demonstrating clinical benefit. Radiological assessments consisted of a total body computed tomography scan, which was performed at baseline, at variable time intervals based on local clinical practice guidelines, and on clinical suspicion of progressive disease (PD). Tumor response was assessed according to RECIST v.1.1, and was defined as complete response (CR), partial response (PR), stable disease (SD), and PD. The objective response rate (ORR) was defined as the sum of CR and PR, while the disease control rate was defined as the sum of CR, PR, and SD.

Table 1  
 Characteristics of patients with aNSCLC by smoking history (smokers or former smokers, S-pts; never-smoking patients, NS-pts)

Clinical characteristic	S-pts N = 111 (%)	NS-pts N = 31 (%)
Age, median (range)	65 (42–82)	62 (38–84)
Sex		
Male	73 (65.8)	15 (48.4)
Female	38 (34.2)	16 (51.6)
Histologic profile		
Squamous	16 (14.4)	3 (9.7)
Nonsquamous	95 (85.6)	28 (90.3)
ECOG performance status		
0–1	103 (92.8)	29 (93.5)
≥ 2	7 (6.2)	2 (6.5)
Not assessed	1 (1)	0
TMB, median (range)	8 (0–55)	4 (0-39.09)
Pathway		
Cell Cycle	50 (45)	14 (45.2)
Hippo	1 (1)	1 (3.2)
Myc	9 (8.1)	3 (9.7)
Notch	13 (11.7)	8 (25.8)
Oxidative Stress/Nrf2	16 (14.4)	7 (22.6)
PI3K	42 (37.8)	7 (22.6)
RTK/RAS/MAP	86 (77.5)	26 (83.9)
TGF-β	2 (1.8)	1 (3.2)
p53	85 (76.6)	23 (74.2)
β-catenin/Wnt	7 (6.3)	5 (16.1)
DDR	21 (18.9)	14 (45.2)
Abbreviations: ECOG, Eastern Cooperative Oncology Group; TMB, tumor mutation burden; DDR, DNA Damage Response and Repair.		

# POPLAR and OAK population

Freely publicly available data from blood-based NGS (bNGS) of the biomarker-evaluable population (BEP) of the phase II POPLAR (NCT01903993) (N = 211) and phase III OAK (NCT02008227) (N = 642) randomized trials were used for external validation (11–13). The POPLAR BEP included 15 patients with an epidermal growth factor receptor (EGFR) mutation or anaplastic lymphoma kinase (ALK) rearrangement and 196 without known alterations. The OAK BEP included 59 patients with an EGFR mutation or ALK rearrangement and 583 without known alterations. Both the POPLAR and OAK studies were performed in full accordance with the guidelines for Good Clinical Practice and the Declaration of Helsinki, and all patients had provided written informed consent. Protocol approvals were obtained from independent ethics committees of each participating site for both studies. Similarities in the design of the POPLAR and OAK trials justified pooling of the data. Both trials included patients with measurable previously treated aNSCLC, unselected for PD-L1 status, and randomly assigned to receive either atezolizumab or docetaxel; both used the same stratification factors and schedule of assessments and crossover was not permitted. In both trials, patients were randomized to intravenous atezolizumab or docetaxel arms in a 1:1 ratio. The primary endpoint was overall survival (OS); progression-free survival (PFS) was one of the secondary endpoints. Detailed descriptions of the eligibility criteria and recruitment methods for both trials have been published previously (12–14). The variables considered were: ECOG PS, gender, smoking history, histology, tumor burden, and start and end date of treatment. Each study team reviewed all axial computed tomographic images according to RECIST v.1.1.

## Targeted next-generation sequencing and oncogenic pathway classification

For the real-world population, NGS analysis was performed on available pretreatment tumor tissue using the FoundationOne®CDx assay (Foundation Medicine, Cambridge, MA, USA).

Alterations reported in the Catalogue of Somatic Mutations in Cancer (COSMIC) and ClinVar databases (15, 16) were identified in both populations (real-world and POPLAR/OAK); the alterations reported as pathogenic by the COSMIC and ClinVar were classified as deleterious. A total of 11 signaling pathways with frequent genetic alterations were evaluated, starting with key cancer genes explored in previous TCGA publications (17). The following pathways were analyzed: (1) cell cycle, (2) Hippo, (3) Myc, (4) Notch, (5) oxidative stress/Nrf2, (6) PI3K, (7) RTK/RAS/MAP, (8) TGF- $\beta$ , (9) p53, (10)  $\beta$ -catenin/Wnt, and (11) DDR. They were used to redefine the mutational profile of patients in terms of mutated pathways: each pathway was labeled “mutated” if the patient manifested at least one mutation in that pathway. All the analyzed genes and pathway member genes considered for the real-world and POPLAR/OAK populations have been listed in **Tables S1b and c**.

## PD-L1 testing and (blood)TMB assessment

The same PD-L1 testing and TMB assessments methods were used in the real-world and POPLAR and OAK populations. PD-L1 expression was reported as the percentage of tumor cells with positive

membranous staining in a slide containing at least 100 tumor viable cells. PD-L1 expression was determined by immunohistochemistry using the Dako PD-L1 22C3 pharmDx assay (Dako, Glostrup, Denmark). TMB, defined as the number of somatic, coding, base substitution, and insertion/deletion (indel) mutations per megabase (Mb) of genome examined, was calculated using the NGS FoundationOne®CDx assay. The blood TMB (bTMB) assay uses the same hybridization-capture methodology as the United States Food and Drug Administration-approved FoundationOne CDx NGS assay and targets 1.1 Mb of genomic coding sequences (18). We used the same variable cut-off of TMB that was used to define high TMB in previous studies (19).

## **Clinical outcomes**

PFS was defined as the time from the start of PD-L1 inhibitor therapy to disease progression or death, whichever occurred first. Patients who were alive without disease progression were censored on the last date of adequate disease assessment. OS was defined as the time from the start of PD-L1 inhibitor therapy to death. Patients who were still alive were censored at the date of last contact.

## **Statistical analysis**

All between-group differences in clinical characteristics and response outcomes were analyzed using the two-tailed Wilcoxon rank sum test and the Kruskal–Wallis test. Enrichment analysis (hypergeometric distribution) was performed to characterize patients' subgroups in terms of mutated pathways. Statistical analyses were also performed with a focus on the sub-cohorts identified based on TMB levels (H-TMB and L-TMB).

## **Patients similarity network analysis**

To further investigate the patients' molecular characterization and the presence of a relationship between signaling pathways, TMB levels, and tobacco use in the real-world population, patient similarity networks were constructed for both smoking patients (smokers or former smokers, S-pts) and never-smoking patients (NS-pts) cohorts. In a patient similarity network, the nodes correspond to the patients and the weighted links between nodes indicate how similar the patients are in terms of specific properties. In this study, the Euclidean distance between mutated pathway profiles of each pair of patients was first computed to assess patient similarity. A scaled exponential similarity kernel was then used to determine the weight of the links (20). Once the network was obtained, community detection (Louvain method) (21, 22) was performed to discover subgroups of patients more similar to each other (network community). The identified communities were finally characterized in terms of clinical characteristics and response outcomes (Kruskal–Wallis test).

### **Literature search strategy and selection criteria**

Finally, to confirm our observations, a systematic literature review was performed on July 23, 2022 to identify published studies evaluating the role of DDR in IO response among patients with lung cancer. Meta-analyses and reviews, registered trials or trials with published protocols lacking published results, and articles not written in English were excluded.



A literature review was performed to identify all relevant studies according to the Preferred Reporting Items for Systematic reviews and meta-analyses (PRISMA) extension statement for Scoping Reviews. A completed PRISMA 2020 checklist was used to illustrate the methodology of our study.

The full list of search terms have been provided in supplementary (S1); a combination of disease characteristics and strategies or drugs were used as search terms. The PubMed, Cochrane Central Register of Clinical Trials, and Web of Science databases were searched.

In addition to observational and retrospective studies, subgroup analyses of prospective trials and in-silico analyses published as full papers or abstracts (if entire reports were not available) were included in the analysis. Two reviewers (PL and MF) independently assessed whether each selected randomized controlled trial met the predetermined criteria; a third reviewer (MO) was consulted in case of disagreement. Additional details regarding the search strategy have been provided in supplementary (S2).

Prespecified data elements were extracted from each trial using a structured data abstraction form; the elements included baseline characteristics, sample size, interventions used, and main results. Two reviewers extracted the data from the included trials (PL and MF) and disagreements were resolved by referring to a third reviewer (MO). A total of 262 publications were identified from the literature search. After removal of duplicates, a total of 164 manuscripts were available for analysis. After reading the title and abstract, 148 publications were selected for extended reading of the text; 20 papers were selected for the current study based on the eligibility criteria. The characteristics of the selected studies are summarized in **Table S2**.

## Results

### **Non-smoking patients with H-TMB in a real-world cohort displayed a peculiar genomic profile characterized by mutations in the DDR pathway**

Overall, 142 patients with aNSCLC were retrospectively enrolled in our real-world cohort between January 2017 and March 2021; they underwent molecular profiling using the NGS FoundationOne®CDx assay.

The patient characteristics are summarized in Table 1. A total of 88 (62%) male and 54 (38%) female patients were enrolled; the average age was 63.35 (SD +/- 10.48) years. Most patients were smokers or former smokers (S-pts, N = 111, 78%), while 31 patients (NS-pts, 22%) had no history of tobacco use. Most tumors were adenocarcinomas (N = 123, 87%); 19 patients (13%) had squamous histology. The median TMB of the total population was 7.57 Mut/Mb. S-pts had a higher median TMB than NS-pts (8 vs. 4 Mut/Mb, respectively) (Fig. 1). Interestingly, among the NS-pts, 11 showed a TMB of higher than 10 Mut/Mb (median TMB: 16.39).

A review of all mutations detected by NGS population analysis in the COSMIC and ClinVar databases enabled the identification of mutations reported as pathogenic. Such pathogenic mutations were subsequently classified into the 11 signaling pathways previously described. Enrichment analysis was

then performed to assess whether specific pathways accumulated a higher frequency of mutations depending on the TMB cut-off (H-TMB vs. L-TMB) or patient smoking history (S-pts vs. NS-pts).

On performing enrichment analysis considering the TMB level, the H-TMB subgroup (53 pts, 37%) had statistically significant enrichments in cell cycle and Notch pathway alterations (p-values = 0.0039 and 0.0032, respectively). On the contrary, no enrichment was identified in the L-TMB cohort (**Table S3a**).

The smoking history, independent of the TMB values, did not appear to be associated with alterations of specific pathways; no significant enrichment of mutations was found in any pathway when comparing S-pts with NS-pts (**Table S3b**).

As previously performed for the general population, enrichment analysis was repeated after stratifying the two cohorts of S-pts and NS-pts based on the level of TMB (H-TMB and L-TMB). Two statistically significant enrichments were identified in the NS/H-TMB cohort. In particular, the highlighted enrichments depended on the  $\beta$ -Catenin/Wnt and the DDR pathways (p-value = 0.0027 and 0.0014, respectively). In particular, 8/11 (73%) NS/H-TMB patients had at least 1 alteration of the DDR pathway (**Table 2**). These results indicated the presence of distinct molecular profiles (depending on the TMB values) in the entire patient population (H-TMB vs L-TMB pts) and within the specific subgroup of NS/H-TMB pts.

## Non-smoking patients with H-TMB showed superior clinical benefit with immune checkpoint treatment

In our series, the cohort of NS-pts showed a significantly higher median OS and median PFS than that of S-pts (p-value = 0.0032 and 0.0018, respectively) despite differences in median TMB (**Fig. 2a,b,c**).

In particular, this difference was driven by the NS/H-TMB subgroup, which was enriched in DDR mutations; this subgroup demonstrated a median OS of 26 months and an ORR of 100% (11/11 patients) (**Fig. 3a,b,c**). These results showed that the NS/ H-TMB subgroup is a homogeneous group that is exceptionally responsive to IO.

## DDR pathway mutations as a molecular feature of NS/H-TMB pts in POPLAR/OAK population

The bNGS data from the BEP of the phase II POPLAR (NCT01903993) and III OAK (NCT02008227) randomized trials were used to confirm whether the NS/H-TMB subgroup was characterized by an enrichment of mutation in the DDR and  $\beta$ -catenin pathways.

The clinical and molecular data of 853 patients were analyzed. Among them, 713 (84%) patients were current or former smokers, while 140 (16%) were non-smokers. The cohorts of S-pts and NS-pts had a median TMB of 9 and 4 Mut/Mb, respectively (**Figure S1a e S1b**). All the pathogenic mutations in the 11 pathways for the POPLAR/OAK cohort were classified and enrichment analyses were performed as previously described.

In the NS cohort, 18 patients were identified to have H-TMB (> 10 Mut/Mb). The analysis performed on the NS/H-TMB population confirmed statistically significant enrichment for mutations in the DDR pathway (p-value = 0.0297). In contrast, no significance was confirmed for the  $\beta$ -Catenin/Wnt pathway (5 of 18 patients, p-value = 0.6129). Interestingly, mutations in the DDR pathway were detected in 17/18 patients from the NS/H-TMB subgroup; 6 patients had more than 1 mutation (2–8 mutations). This analysis confirmed the observation that the NS/H-TMB population was characterized by a specific mutation enrichment in the DDR pathway.

## Network analysis for patient similarity evaluation

The patient similarity network was built and analyzed to further investigate the molecular characterization of the NS-pts of our cohort (31 pts) (Fig. 4). A total of 4 communities were obtained, each characterized by a mutated pathway profile. The first subgroup (NS C1) comprised 8 patients, all with a TMB level above the threshold of 10 Mut/Mb; patient similarity was observed due to the mutation of several pathways in more than half of the patients (Fig. 4a, bottom). The pathways were as follows: cell cycle (7/8 pts), RTK/RAS/MAP (7/8 pts), p53 (7/8 pts), Notch (6/8 pts), DDR (6/8 pts), oxidative stress/Nrf2 (5/8 pts), and  $\beta$ -catenin/Wnt (5/8 pts). The second community (NS C2, 4 pts) showed a clear pattern of similarity; all patients had at least one mutation in both RTK/RAS/MAP and p53 pathways. The main feature that characterized the 7 patients of the third community (NS C3) was the presence of mutations in the cell cycle, RTK/RAS/MAP, and p53 pathways in all patients (100%). Finally, the fourth community (NS C4, 12 pts) was the weakest in terms of a clear profile of mutated pathways. The highest percentage of patients shared at least 1 mutation of the RTK/RAS/MAP pathway (8/12 pts); the other percentages were below 50% (the details are presented in **Fig. 4a**, bottom). Lastly, it is worth noting that the NS C1 community showed a significantly higher TMB level than the other communities (p-value = 0.0025; **Fig. 5b**).

An interesting trend emerged in terms of OS: patients in NS C1 (8 pts with significantly higher TMB values) and NS C2 (only 4 pts) showed a higher OS level than that of patients in the other communities (p-value = 0.0953; **Fig. 4c**); however, no significant trend emerged in terms of PFS (p-value = 0.7416).

Similarity network analysis in the S-pts population also yielded four communities (**Fig. 5**) that shared commonly mutated pathways. The S C1 community (12 pts) was characterized by mutations in the cell cycle, RTK/RAS/MAP, and p53 pathways in all patients. In addition to these pathways, the PI3K pathway was also found to be mutated in the S C3 community (8 pts, 100% mutated). The S C2 community (14 pts) conserved mutations in the RTK/RAS/MAP and p53 pathways and the S C4 community (77 pts) did not show a clear mutated pathway profile; the highest percentages of patients shared mutations in the RTK/RAS/MAP (67.53%; 52/77 pts) and p53 (66.23%; 51/77 pts) pathways.

However, none of these communities were characterized by a significantly higher level of TMB; the threshold of 10 Mut/Mb was also not consistent (i.e., all patients with a TMB level above the threshold, as in NS C1). It is interesting to note that the S C2 community demonstrated a lower TMB than the S C3 and

S C4 communities (p-value = 0.0422) (Fig. 5b). No significant trend emerged among the communities in terms of OS (p-value = 0.9539) (Fig. 5c) and PFS (p-value = 0.774).

Network analysis therefore identified different patterns of patient communities based on their molecular features and smoking status.

## Discussion

This study on a real-world cohort of aNSCLC with PD-L1  $\geq$  50% identified a subgroup of NS-pts enriched with deleterious DDR mutations. This subgroup had H-TMB and demonstrated improved clinical outcomes with first-line pembrolizumab, unlike non-smoking patients, who usually have a L-TMB and are unresponsive to IO.

To our knowledge, this is the first real-world report that identified a particular molecular subgroup in a treatment-naïve population of aNSCLC with PD-L1  $\geq$  50% and also the first to use a patient similarity network for identifying different patient communities based on their molecular features and smoking status.

These results were reproduced in an external cohort using POPLAR/OAK data, confirming that the subgroup of NS-pts with H-TMB was responsive to immunotherapy.

Numerous papers have previously described the role of DDR mutations as predictors of response to IO (3–10; 23). Our literature review demonstrated that the vast majority of evidence in this field consists of retrospective and/or in-silico analyses. In general, (except for PALB2 and the conflicting data regarding ARID1A) alterations in genes related to DDR, HRR, and the MMR systems appear to be predictive factors for response to immunotherapy in lung cancer patients. However, these data are of suboptimal quality and almost all studies did not primarily aim to demonstrate a relationship between the DDR pathway and IO response. In addition, these studies analyzed DDR alterations in the entire population and did not identify particular enrichments in the non-smoking population.

Although the close relationship between lung cancer and smoking has long been known, the mechanisms that induce the disease in non-smoking patients are considerably less well-known. It is important to note that unlike S-NSCLCs, NS-NSCLCs are becoming increasingly commoner worldwide. New data providing a possible etiological mechanism for EGFR-mutant NS-NSCLC have recently been presented (24). However, a deeper understanding of carcinogenesis and molecular reclassification of NS-NSCLCs remain significant unmet clinical needs.

NS-aNSCLCs are usually characterized by few driver mutations and a L-TMB. These characteristics make IO treatments ineffective and often counterproductive. On the contrary, the molecular subgroup of NS-pts with H-TMB, identified in this study, did not show driver mutations, but a widespread genomic instability in the DDR pathway. These alterations could be the critical event explaining the occurrence of

carcinogenesis without other risk factors (i.e., smoking and mutations in driver genes such as *EGFR* and *ALK*) and could identify a subgroup of aNSCLC prone to genomic instability.

The increasing diffusion of comprehensive genome profiles could help identify and characterize this subgroup in detail. It was not possible to determine specific and recurrent mutations of the DDR pathway in our analysis due to the small sample size. Our study has certain limitations. It had a retrospective and monocentric design, the number of NS/H-TMB patients was low, and data from paired germline analyses were not available for verifying any germline alterations of the DDR pathway. Despite these limitations, we believe that the described results may be biologically and clinically relevant.

DDR mutations of this subgroup should not only be considered as a proxy of H-TMB, but as a possible key event in carcinogenesis. Indeed, patient similarity network analysis allowed NS-pts with mutated DDR pathways to be grouped in a distinct community than other communities of NS-pts.

The identification of this molecular cohort could also have further therapeutic implications. In fact, various molecules targeting the DDR pathway, such as PARP and ATR inhibitors, are being recently developed; these molecules are being administered alone or in combination with immunotherapeutic agents in solid tumors (25–27).

In conclusion, our analysis identified a molecular subgroup of aNSCLC NS/H-TMB patients with alterations of the DDR pathway that was potentially responsive to IO. This may represent a novel signature for better selection of NS-pts with non-oncogene addicted aNSCLC and  $PD-L1 \geq 50\%$  for IO treatment. Further larger multi-centric prospective studies are needed to confirm our data in order to explore the role of DDR pathogenic mutation in patients candidate to receive IO single agent or in combination with chemotherapy and to implement these findings in clinical practice. Further studies on large cohorts may improve patient benefit from immunotherapy in the future.

## Abbreviations

aNSCLC: non-oncogene addicted advanced non-small cell lung cancer

TMB: tumor mutation burden

IO: immunotherapy

H-TMB: high TMB

S-pts: smoking patient

NS-pts. never-smoking patients

L-TMB: low TMB

DDR: DNA damage response and repair

ECOG PS: Eastern Cooperative Oncology Group performance status score

RECIST: Response Evaluation Criteria in Solid Tumors

NGS; next generation sequencing

PD: progressive disease

CR: complete response

PR: partial response

SD: stable disease

ORR: objective response rate

bNGS: blood-based NGS

BEP: biomarker-evaluable population

OS: overall survival

PFS: progression-free survival

EGFR: epidermal growth factor receptor

ALK: anaplastic lymphoma kinase

COSMIC: Catalogue of Somatic Mutations in Cancer

Mb: megabase

bTMB: blood TMB (bTMB)

## **Declarations**

### **Disclosure of potential conflicts of interest**

### **Authors' contributions**

Conception and design: Marco Filetti, Mario Occhipinti, Lorenzo Farina, Aurelia Rughetti, Manuela Petti.

Development of methodology: Marco Filetti, Mario Occhipinti, Lorenzo Farina, Aurelia Rughetti, Manuela Petti.

Acquisition of data (provided animals, acquired and managed patients, provided facilities, etc.): Marco Filetti, Mario Occhipinti, Alessio Cirillo, Fabio Scirocchi, Alessio Ugolini, Raffaele Giusti

Analysis and interpretation of data (e.g., statistical analysis, biostatistics, computational analysis): Marco Filetti, Manuela Petti, Pasquale Lombardi, Lorenzo Farina

Writing, review, and/or revision of the manuscript: Marco Filetti, Mario Occhipinti, Alessio Cirillo,

Administrative, technical, or material support (i.e., reporting or organizing data, constructing databases): Marco Filetti, Mario Occhipinti, Alessio Cirillo, Manuela Petti, Lorenzo Farina

Study supervision: Andrea Botticelli, Giuseppe Lo Russo, Filippo Maria De Braud, Paolo Marchetti, Gennaro Daniele, Marianna Nuti, Elisabetta Ferretti, Aurelia Rughetti, Lorenzo Farina

## Funding

This work was partially supported by funding to MF (Sapienza research grant number: AR12218166B9BEFB)

## References

1. Reck M, Rodríguez-Abreu D, Robinson AG, Hui R, Csósz T, Fülöp A, *et al.* Updated analysis of KEYNOTE-024: Pembrolizumab versus platinum-based chemotherapy for advanced non-small-cell lung cancer with PD-L1 tumor proportion score of 50% or greater. *J Clin Oncol* 2019;37:537–46.
2. Samstein RM, Lee CH, Shoushtari AN, Hellmann MD, Shen R, Janjigian YY, *et al.* Tumor mutational load predicts survival after immunotherapy across multiple cancer types. *Nat Genet* 2019;51:202–6.
3. Ricciuti B, Wang X, Alessi JV, Rizvi H, Mahadevan NR, Li YY, *et al.* Association of high tumor mutation burden in non-small cell lung cancers with increased immune infiltration and improved clinical outcomes of PD-L1 blockade across PD-L1 expression levels. *JAMA Oncol* 2022;16:e221981.
4. Gainor JF, Rizvi H, Jimenez Aguilar E, Skoulidis F, Yeap BY, Naidoo J, *et al.* Clinical activity of programmed cell death 1 (PD-1) blockade in never, light, and heavy smokers with non-small-cell lung cancer and PD-L1 expression  $\geq 50$ . *Ann Oncol.* 2020 Mar;31(3):404–411.
5. Fang W, Zhou H, Shen J, Li J, Zhang Y, Hong S, Zhang L. MDM2/4 amplification predicts poor response to immune checkpoint inhibitors: a pan-cancer analysis. *ESMO Open.* 2020;5(1):e000614.
6. Mouw KW, Goldberg MS, Konstantinopoulos PA, D'Andrea AD. DNA damage and repair biomarkers of immunotherapy response. *Cancer Discov* 2017;7:675–93.
7. Strickland KC, Howitt BE, Shukla SA, Rodig S, Ritterhouse LL, Liu JF, *et al.* Association and prognostic significance of BRCA1/2-mutation status with neoantigen load, number of tumor-infiltrating lymphocytes and expression of PD-1/PD-L1 in high grade serous ovarian cancer. *Oncotarget* 2016;7:13587–98.
8. Rizvi NA, Hellmann MD, Snyder A, Kvistborg P, Makarov V, Havel JJ, *et al.* Mutational landscape determines sensitivity to PD-1 blockade in non-small cell lung cancer. *Science* 2015;348:124–8.

9. Chae YK, Davis AA, Raparia K, Agte S, Pan A, Mohindra N, *et al.* Association of tumor mutational burden with DNA repair mutations and response to anti-PD-1/PD-L1 therapy in non-small-cell lung cancer. *Clin Lung Cancer* 2019;20:88–96.
10. Ricciuti B, Recondo G, Spurr LF, Li YY, Lamberti G, Venkatraman D, *et al.* Impact of DNA damage response and repair (DDR) gene mutations on efficacy of PD-(L)1 immune checkpoint inhibition in non-small cell lung cancer. *Clin Cancer Res* 2020;26:4135–42.
11. Gandara DR, Paul SM, Kowanetz M, Schleifman E, Zou W, Li Y, *et al.* Blood-based tumor mutational burden as a predictor of clinical benefit in non-small-cell lung cancer patients treated with atezolizumab. *Nat Med* 2018;24:1441–8.
12. Fehrenbacher L, Spira A, Ballinger M, Kowanetz M, Vansteenkiste J, Mazieres J, *et al.* POPLAR Study Group. Atezolizumab vs. docetaxel for patients with previously treated non-small-cell lung cancer (POPLAR): a multicentre, open-label, phase 2 randomised controlled trial. *Lancet* 2016;387:1837–46.
13. Rittmeyer A, Barlesi F, Waterkamp D, Park K, Ciardiello F, von Pawel J, *et al.* OAK Study Group. Atezolizumab vs. docetaxel in patients with previously treated non-small-cell lung cancer (OAK): a phase 3, open-label, multicentre randomised controlled trial. *Lancet* 2017;389:255–65.
14. Fehrenbacher L, von Pawel J, Park K, Rittmeyer A, Gandara DR, Ponce Aix S, *et al.* Updated efficacy analysis including secondary population results for OAK: a randomized phase III study of atezolizumab vs. docetaxel in patients with previously treated advanced non-small cell lung cancer. *J Thorac Oncol* 2018;13:1156–70.
15. Forbes SA, Beare D, Boutselakis H, Bamford S, Bindal N, Tate J, *et al.* COSMIC: somatic cancer genetics at high-resolution. *Nucleic Acids Res* 2017;45:D777–83.
16. Landrum MJ, Lee JM, Benson M, Brown G, Chao C, Chitipiralla S, *et al.* ClinVar: public archive of interpretations of clinically relevant variants. *Nucleic Acids Res* 2016;44:D862–8.
17. Sanchez-Vega F, Mina M, Armenia J, Chatila WK, Luna A, La KC, *et al.* Cancer Genome Atlas Research Network; Van Allen EM, Cherniack AD, Ciriello G, Sander C, Schultz N. Oncogenic Signaling Pathways in The Cancer Genome Atlas. *Cell*. 2018 Apr 5;173(2):321–337.e10.
18. Frampton GM, Fichtenholtz A, Otto GA, Wang K, Downing SR, He J, *et al.* Development and validation of a clinical cancer genomic profiling test based on massively parallel DNA sequencing. *Nat Biotechnol* 2013;31:1023–31.
19. Büttner R, Longshore JW, López-Ríos F, Merkelbach-Bruse S, Normanno N, Rouleau E, *et al.* Implementing TMB measurement in clinical practice: considerations on assay requirements. *ESMO Open*. 2019;4(1):e000442.
20. Wang B, Mezlini AM, Demir F, Fiume M, Tu Z, Brudno M, *et al.* Similarity network fusion for aggregating data types on a genomic scale. *Nat Methods* 2014;11:333–7.
21. Blondel VD, Guillaume JL, Lambiotte R, Lefebvre E. Fast unfolding of communities in large networks. *J Stat Mech* 2008;2008:P10008.
22. Rahiminejad S, Maurya MR, Subramaniam S. Topological and functional comparison of community detection algorithms in biological networks. *BMC Bioinformatics* 2019;20:212.



23. Cortellini A, Giusti R, Filetti M, Citarella F, Adamo V, Santini D *et al*. High familial burden of cancer correlates with improved outcome from immunotherapy in patients with NSCLC independent of somatic DNA damage response gene status. *J Hematol Oncol*. 2022 Jan 21;15(1):9.
24. Lim E, Hill W, Lee C, Weeden CE, Augustine M, Chen K, *et al*. 1MO Air pollution-induced non-small cell lung cancer: Towards molecular cancer prevention, *Annals of Oncology*, Volume 33, Supplement 8, 2022, Page S1383.
25. Musacchio L, Cicala CM, Camarda F, Ghizzoni V, Giudice E, Carbone MV, *et al*. Combining PARP inhibition and immune checkpoint blockade in ovarian cancer patients: a new perspective on the horizon? *ESMO Open* 2022;7:100536.
26. Wanderley CWS, Correa TS, Scaranti M, Cunha FQ, Barroso-Sousa R. Targeting PARP1 to enhance anticancer checkpoint immunotherapy response: rationale and clinical implications. *Front Immunol* 2022;13:816642.
27. Ngoi NYL, Peng G, Yap TA. A tale of two checkpoints: ATR inhibition and PD-(L)1 blockade. *Annu Rev Med* 2022;73:231–50.

## Tables

Table 2 is available in the Supplementary Files section.

## Figures

**Figure 1.** Overall population: violin plot TMB according to smoking status.

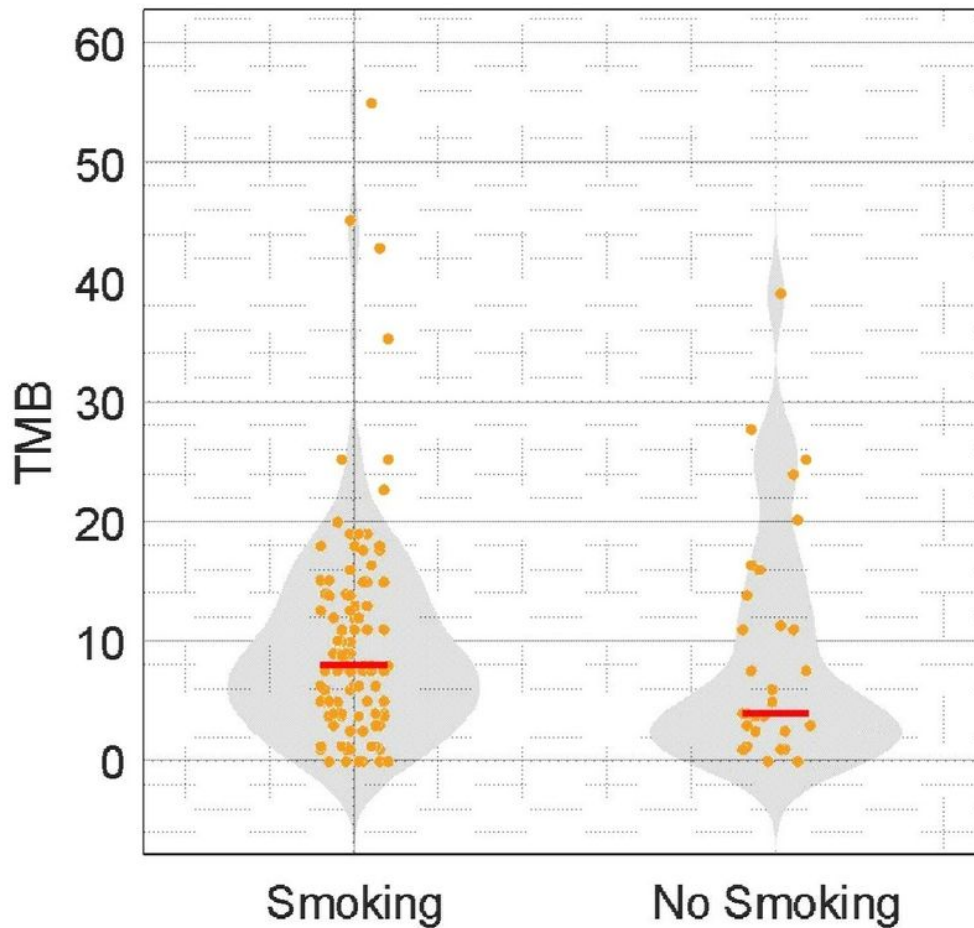


**Figure 1**

See image above for figure legend.

**Figure 2a,b,c.** Overall population: OS, PFS and ORR according to smoking status.

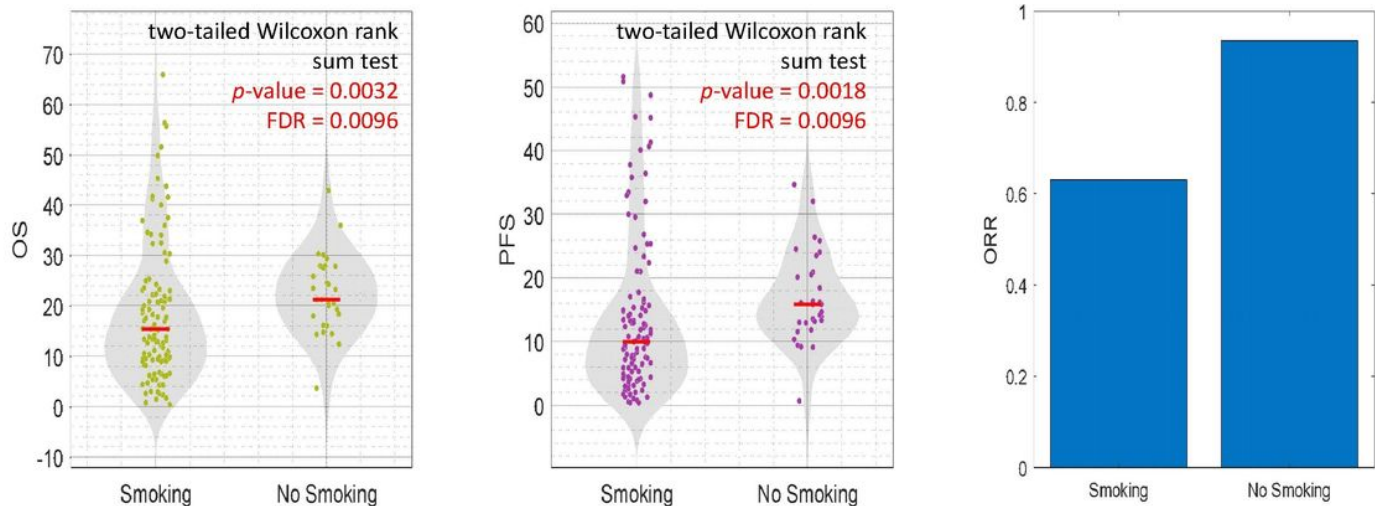


**Figure 2**

See image above for figure legend.

**Figure 3a,b,c.** H-TMB population: OS, PFS and ORR according to smoking status.

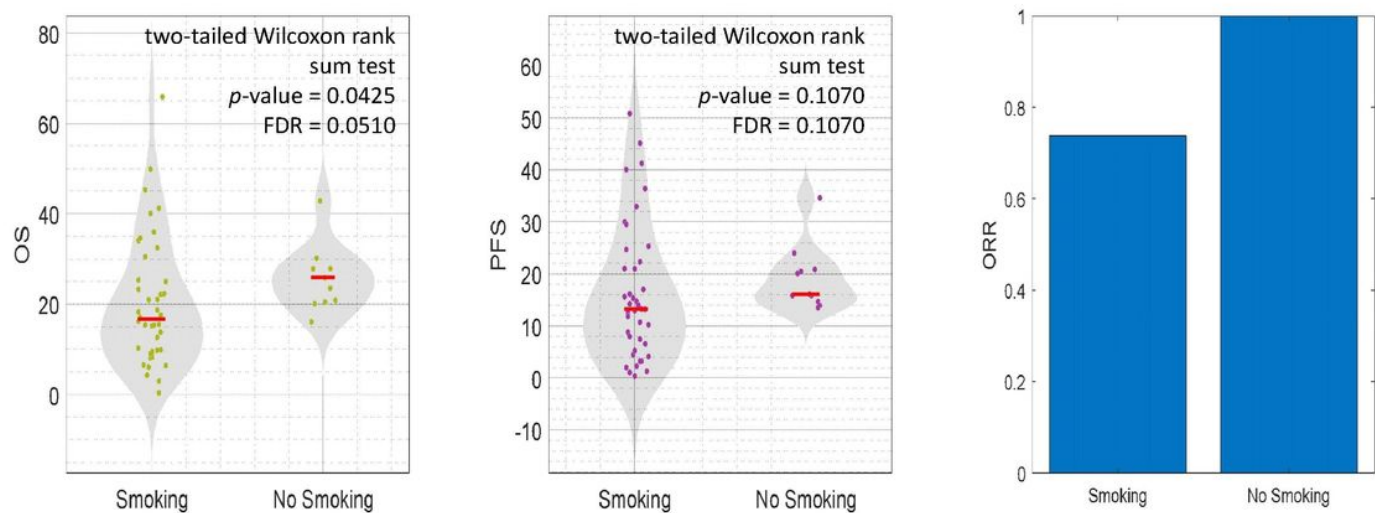
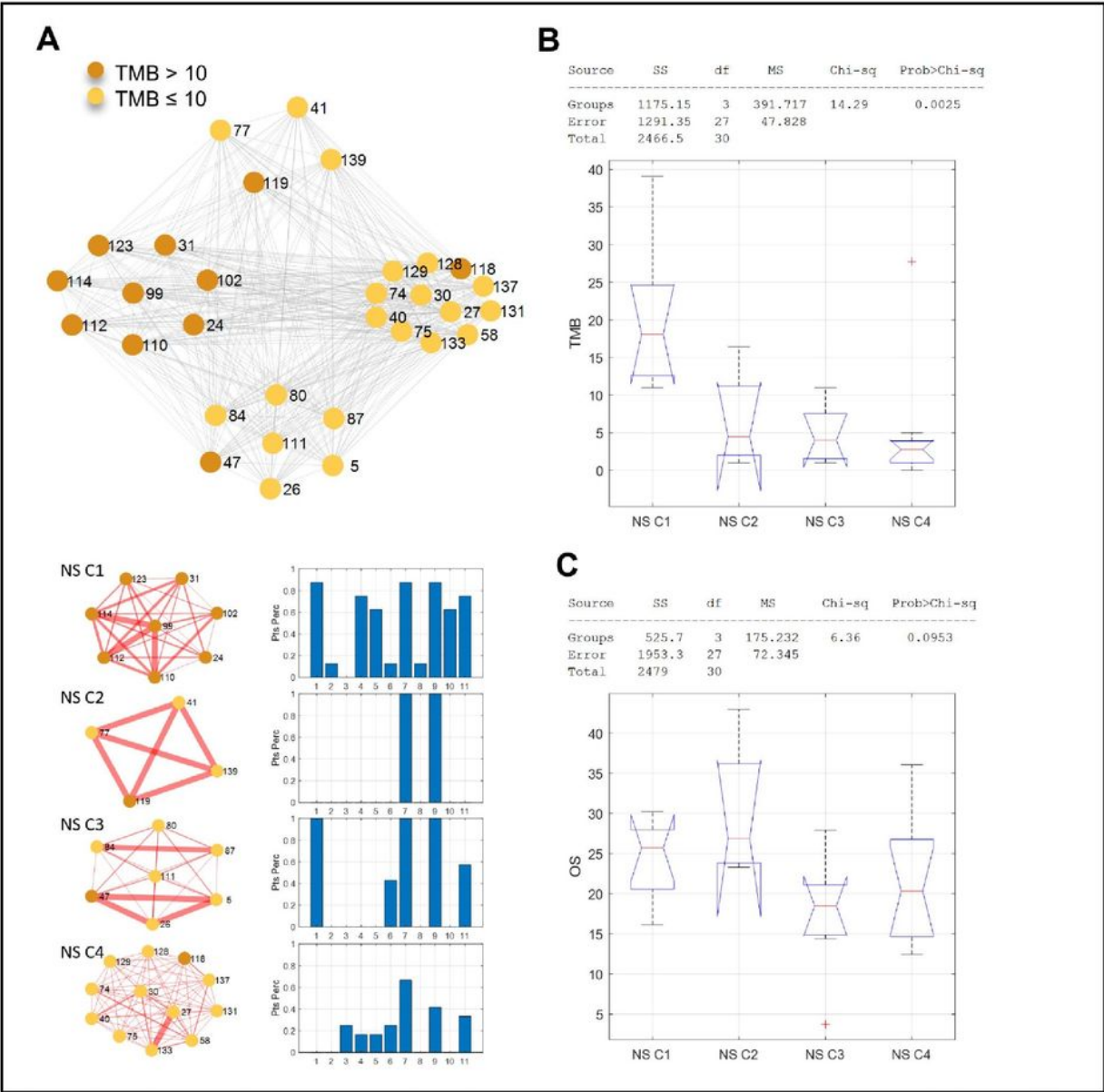


Figure 3

See image above for figure legend.



**Figure 4. A.** Patient similarity network of the never-smoking cohort. Nodes color codes for the TMB level: orange for TMB > 10 Mut/Mb, yellow for TMB ≤ 10 Mut/Mb. In the bottom of the panel, the four identified communities are shown with the associated mutated pathways profile: bar diagrams of the percentage of patients characterized by at least one mutation in each of the analyzed pathways (1-Cell cycle-pathway, 2-Hippo pathway, 3-Myc pathway, 4-Notch pathway, 5-Oxidative stress/Nrf2 pathway, 6-PI3K pathway, 7-RTK/RAS/MAP pathway, 8-TGF beta pathway, 9-p53 pathway, 10-beta-catenin/Wnt pathway, 11-DDR pathway). **B.** Kruskal–Wallis test results on effect of TMB. **C.** Kruskal–Wallis test results on effect of OS.

Figure 4

See image above for figure legend.

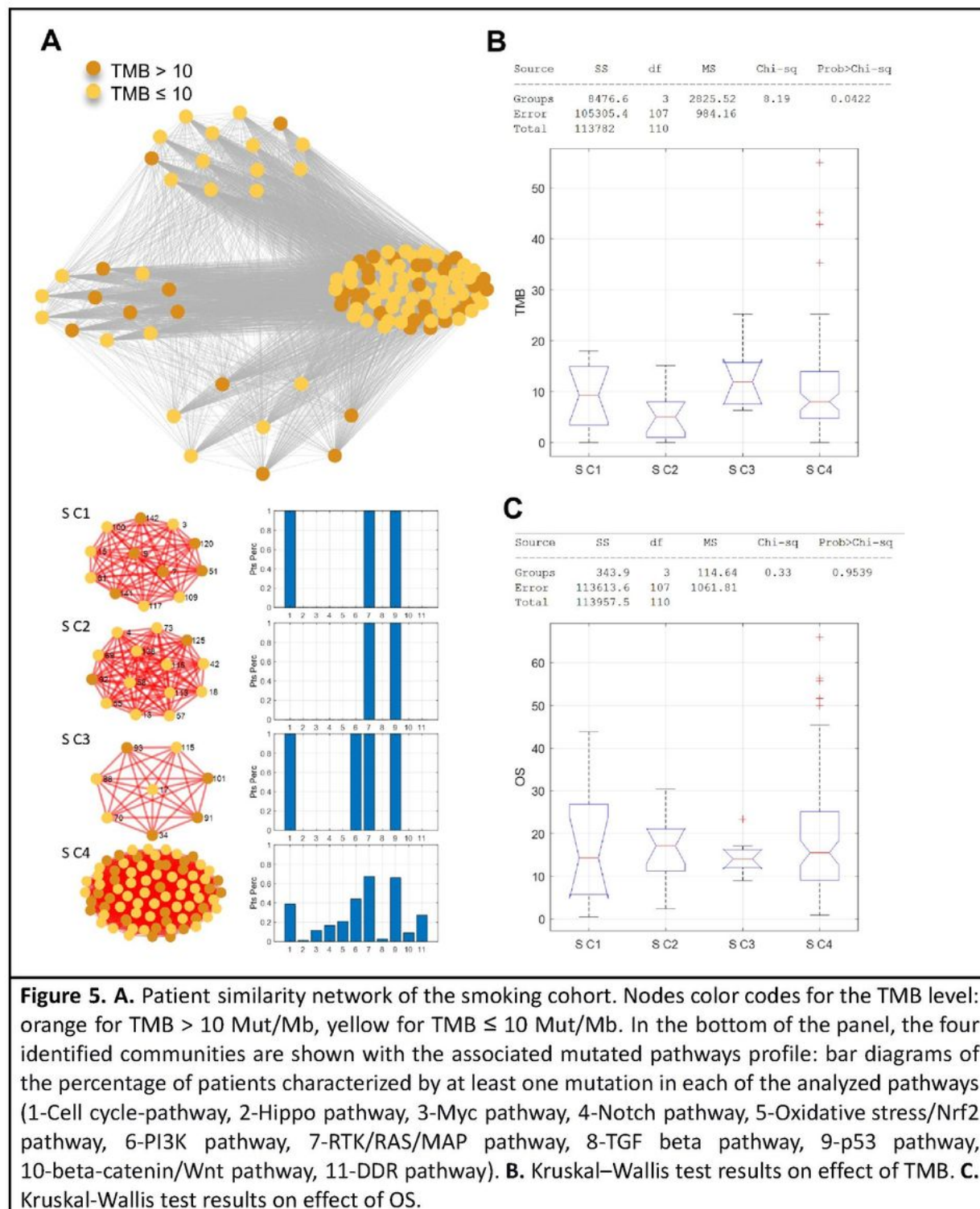


**Figure 5**

See image above for figure legend.

## Supplementary Files

This is a list of supplementary files associated with this preprint. Click to download.

- Table2.pdf
- FigureS1aandS1b.pptx.pdf
- TableS1aS1bandS1c.pdf
- TableS2.docx.pdf
- TableS3a.pptx.pdf
- TableS3b.pptx.pdf
- S1.docx.pdf
- S2.docx.pdf